

EXIT Chart Based System Design for Iterative Source-Channel Decoding with Fixed-Length Codes

Laurent Schmalen, Marc Adrat, Thorsten Clevorn, and Peter Vary, *Fellow, IEEE*

Abstract—Audio-visual source encoders for digital wireless communications extract parameter sets on a frame-by-frame basis. Due to delay and complexity constraints these parameters exhibit some residual redundancy which manifests itself in non-uniform parameter distributions and intra- as well as inter-frame correlation. This residual redundancy can be exploited by iterative source-channel decoding (ISCD) to improve the robustness against impairments from the channel. In the design process of ISCD systems the well known EXIT charts play a key role. However, in case of inter-frame parameter correlation, the classic EXIT charts do not provide reliable bounds for predicting the convergence behavior of ISCD. We explain the reasons for the so-called overshooting effect and propose a novel extension to the EXIT chart computation which provide significantly better bounds for the decoding trajectories. Four advanced ISCD system configurations are proposed and investigated using the benefits of the improved EXIT chart based system design. These configurations include regular and irregular redundant index assignments. In addition, we incorporate unequal error protection in the optimization of irregular index assignments. We show how to realize a versatile multi-mode ISCD scheme which operates close to the theoretical limit.

Index Terms—Iterative Source-Channel Decoding (ISCD), Soft Decision Source Decoding (SDSD), Turbo Principle, EXIT Chart.

I. INTRODUCTION

THE design of digital wireless communication systems always comprises a trade-off between coding efficiency and error robustness. Usually, some residual redundancy remains after source encoding due to delay and complexity constraints. This natural redundancy manifests itself in non-uniform parameter distributions and intra- as well as inter-frame correlation. It can be exploited at the receiver to increase the error robustness, e.g., [1]–[3].

In this paper, we consider iterative source-channel decoding (ISCD) [4]–[8], which originated from source controlled

This work was supported by the Institute of Communication Systems and Data Processing at RWTH Aachen University, Aachen, Germany. This work was financed partly by the European Union project *FlexCode* under grant FP6-2002-IST-C 020023-2 and partly by the German research cluster of excellence UMIC.

L. Schmalen is now with Alcatel-Lucent Bell Labs, Stuttgart, Germany (email: Laurent.Schmalen@alcatel-lucent.com).

M. Adrat is with the Fraunhofer FKIE, Wachtberg, Germany (email: marc.adrat@fkie.fraunhofer.de).

T. Clevorn is with Intel, Duisburg, Germany (email: thorsten.clevorn@intel.com).

P. Vary is with the Institute of Communication Systems and Data Processing (IND), RWTH Aachen University, Aachen, Germany (email: vary@ind.rwth-aachen.de).

Parts of this paper have been published in M. Adrat, M. Antweiler, L. Schmalen, P. Vary, and T. Clevorn, “On the Overshooting Effect in EXIT Charts of Iterative Source-Channel Decoding,” *IEEE International Conference on Communications*, May 2010.

channel decoding [2], [9]. In each decoding step of ISCD, the source statistics are used to iteratively refine the extrinsic reliabilities in a Turbo like process [10]. A transmission scheme using ISCD can be considered as a concatenation of a soft-input/soft-output (SISO) channel decoder and a softbit or soft-decision source decoder (SDSD) [3]. In the literature, ISCD has been applied to systems employing variable-length codes (VLCs) and fixed-length codes (FLCs). The VLC case, in which ISCD improves the segmentation of the bit stream at the receiver, is not the topic of this article and we refer to the literature for more details, e.g. [11]–[13]. In this paper we focus on FLCs. The benefits of ISCD with FLCs have successfully been demonstrated for several applications such as GSM and wide band adaptive multi-rate (WB-AMR) speech transmission [14], [15] and image/video transmission [16]–[18].

The EXIT chart [19] technique is a well-known analysis and optimization tool for Turbo-like systems [19]–[21] such as ISCD. However, for ISCD system designs exploiting inter-frame correlation [8], [22], [23], the EXIT decoding trajectory “overshoots” the EXIT characteristics of SDSD, e.g. [24], [25], especially during the first iterations. We give reasons for this overshooting effect [25] and we propose a novel extension for determining an EXIT decoding trajectory bound of SDSD.

The EXIT chart technique and its new trajectory bound extension is applied in design and analysis of several advanced ISCD system configurations. It is shown that redundant index assignments may outperform conventional non-redundant index assignments in the context of ISCD [17], [22], [23], [26]. Using EXIT charts and the concept of irregular codes [20], [21], we design capacity-achieving ISCD systems by employing irregular index assignments [27]. Unequal error protection can be effectively incorporated into this concept. Finally, we propose a versatile multi-mode system based on ISCD.

All presented system configurations use convolutional codes as inner channel coding component. Instead of convolutional codes, all kind of channel codes, for example block codes [26], low-density parity-check (LDPC) codes [28], [29], or Turbo codes [30], [31], are applicable as long as the respective SISO decoder is able to generate extrinsic information. The design rule in [32] recommends a recursive inner code for serially concatenated systems.

The paper is structured as follows. In Section II we briefly review the ISCD principle. In Section III we explain the reason

for the overshooting effect and propose the novel extension for determining the EXIT trajectory bound. In Section IV, advanced ISCD system configurations are derived using the extended EXIT chart approach.

II. THE ISCD PRINCIPLE

A. Transmitter

We consider the ISCD transmission scheme of Figure 1. A parametric source encoder extracts a parameter vector \underline{v}_k from the k -th segment of the input signal. The vector \underline{v}_k shall consist of M scalar source codec parameters $v_{m,k}$, $m = 1, \dots, M$. The M source codec parameters $v_{m,k}$ are individually quantized to quantizer reproduction levels $\bar{v}_{m,k} \in \mathbb{V}_m$. The quantizer code books \mathbb{V}_m of size $|\mathbb{V}_m|$ are fixed. Usually, $w_m = \log_2(|\mathbb{V}_m|)$ quantifies the length of the bit pattern $\mathbf{x}_{m,k} = \Phi_m(\bar{v}_{m,k})$ after index assignment and bit mapping, i.e., $\mathbf{x}_{m,k}$ consists of w_m (bipolar) bits $x_{m,k}(l) \in \{+1, -1\}$ with $l = 1, \dots, w_m$. The bit patterns usually exhibit some natural residual source redundancy (parameter distribution, correlation) which can be quantified by the conditional probability mass function¹ $P(\mathbf{x}_{m,k} | \mathbf{x}_{m,k-1})$. The complete frame of bit patterns representing the vector \underline{v}_k is denoted as $\underline{\mathbf{x}}_{m,k} = (\mathbf{x}_{1,k}, \dots, \mathbf{x}_{M,k})$.

For convenience, we assume in what follows that the quantizer code books and index assignments are the same for all M source codec parameters $v_{m,k}$, i.e. we can write $\mathbb{V} = \mathbb{V}_m$, $w = w_m$, and $\Phi(\cdot) = \Phi_m(\cdot)$ for all $m = 1, \dots, M$. Moreover, wherever possible without risk of confusion we skip the indices for time k , position m , and bit l .

Next, a block-type bit interleaver Π of size $M \cdot w$ is applied to a frame $\underline{\mathbf{x}}_k$ of bit patterns. If an additional delay is tolerable, the interleaver can also be applied to several consecutive frames [8], however, this case is not considered here. In what follows, the notation will always refer to the deinterleaved domain if there is no risk of confusion.

Finally, a channel code of rate r_{CC} expands the interleaved frame $\underline{\mathbf{x}}_k$ of bit patterns to a sequence $\underline{\mathbf{y}}_k$ of size Mw/r_{CC} with code bits $y(l)$, $l = 1, \dots, Mw/r_{CC}$. As already mentioned, we restrict our considerations to convolutional codes.

The individual code bits y are BPSK-modulated with symbol energy E_s and transmitted over a memoryless AWGN channel with noise power spectral density $N_0/2$.

B. Receiver with ISCD

The aim of *iterative source-channel decoding* (ISCD) is to determine the *a posteriori* L -values [10] $L(x|\underline{\mathbf{z}})$ for a single data bit x given the complete history of received sequences $\underline{\mathbf{z}}$. For this purpose, channel-related L -values $L(z|y)$ (or $L(z|x)$ in case of a systematic bit, respectively) are jointly exploited with the artificial redundancy from channel coding as well as the natural residual source redundancy on parameter level (distribution, correlation). The signal flow from $L(z|y)$ (or $L(z|x)$, respectively) to $L(x|\underline{\mathbf{z}})$ is illustrated in Fig. 1. A detailed derivation and description of the ISCD receiver can be

¹The ISCD algorithm can easily be extended to consider cross-correlation in adjacent positions m , i.e. to $P(\mathbf{x}_{m,k} | \mathbf{x}_{m-1,k})$, as well, e.g., [16].

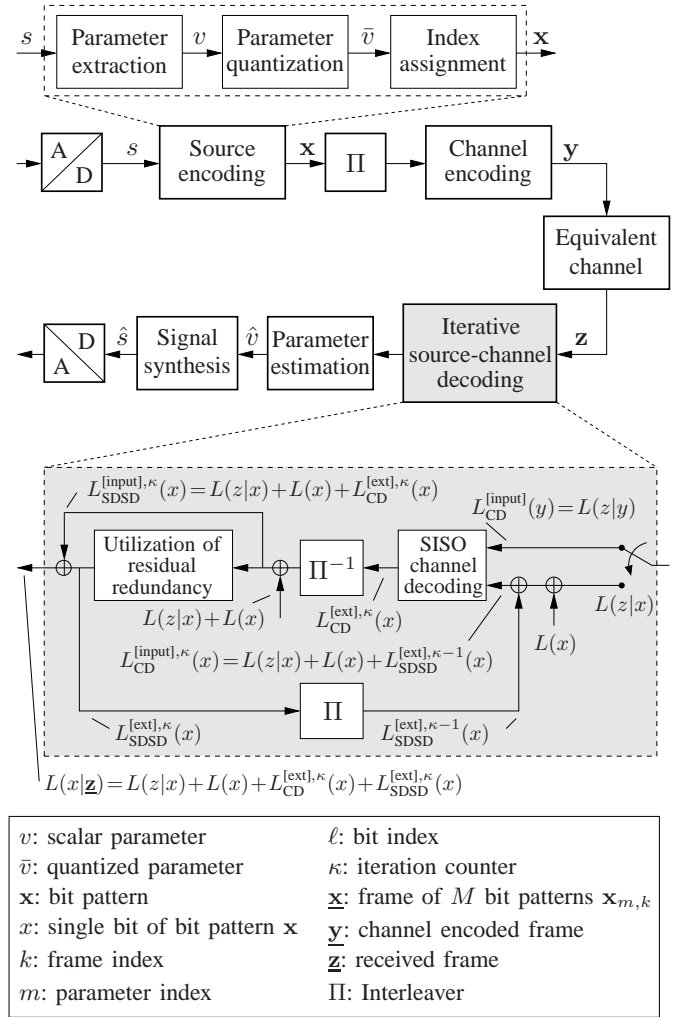


Fig. 1. Block diagram for a transmission system with ISCD.

found in the literature, e.g. [6]–[8]. The term $L(x)$ quantifies the bitwise *a priori* information which determines whether a data bit $x = +1$ or $x = -1$ is more likely.

The two terms $L_{CD/SDS}^{ext,\kappa}(x)$ mark so-called extrinsic information [6], [10] and result from the evaluation of the natural residual source redundancy (labeled with “SDSD”, soft decision source decoding) and of the artificial channel coding redundancy (labeled with “CD”). Here, κ denotes the iteration counter. Concepts how to determine the extrinsic output L -value $L_{CD}^{ext,\kappa}(x)$ of soft-input / soft-output (SISO) channel decoding from the channel-related inputs $L(z|x)$ resp. $L(z|y)$, the bit-wise *a priori* information $L(x)$ and the extrinsic information provided by an outer decoder are well known [10].

C. Extrinsic L -value of Soft Decision Source Decoding

The determination rule for the extrinsic L -value $L_{SDSD}^{ext,\kappa}(x)$ of SDSD shall briefly be reviewed next as it is essential to understand the “overshooting” effect in the EXIT chart of ISCD, which will be discussed in detail in Section III-B. The rule is based on the BCJR algorithm [33].

Updates in the iteration κ (fixed frame index k): The determination of $L_{SDSD}^{ext,\kappa}(x)$ for an arbitrary but fixed bit x

at iteration step κ is given by

$$L_{\text{SDSD}}^{[\text{ext}],\kappa}(x(l_x)) = \frac{\sum_{\mathbf{x}_k^{[\text{ext}]}} \sum_{\mathbf{x}_{k-1}} \gamma_k^{[\text{ext}],\kappa}(\mathbf{x}_k^{[\text{ext}]}, \mathbf{x}_{k-1} | x_k(l_x) = +1) \cdot \alpha_{k-1}(\mathbf{x}_{k-1})}{\log \frac{\sum_{\mathbf{x}_k^{[\text{ext}]}} \sum_{\mathbf{x}_{k-1}} \gamma_k^{[\text{ext}],\kappa}(\mathbf{x}_k^{[\text{ext}]}, \mathbf{x}_{k-1} | x_k(l_x) = -1) \cdot \alpha_{k-1}(\mathbf{x}_{k-1})}. \quad (1)$$

The outer summation in (1) runs over all $2^{w-1} = |\mathbb{V}|/2$ possible realizations of $\mathbf{x}_k^{[\text{ext}]}$ which stands for the bit pattern \mathbf{x}_k excluding the data bit $x_k(l_x)$ under consideration. The inner summation runs over all $2^w = |\mathbb{V}|$ possible realizations of \mathbf{x}_{k-1} . The extrinsic innovation is given by

$$\gamma_k^{[\text{ext}],\kappa}(\mathbf{x}_k^{[\text{ext}]}, \mathbf{x}_{k-1} | x_k(l_x)) = P(\mathbf{x}_k^{[\text{ext}]}, \mathbf{x}_{k-1} | x_k(l_x)) \cdot \exp \sum_{\substack{l=1 \\ l \neq l_x}}^w \frac{x(l)}{2} \cdot L_{\text{SDSD}}^{[\text{input}],\kappa}(x(l)). \quad (2)$$

The term $P(\mathbf{x}_k^{[\text{ext}]}, \mathbf{x}_{k-1} | x_k(l_x))$ can be derived from the conditional probability $P(\mathbf{x}_k | \mathbf{x}_{k-1})$. Note, the bit under consideration $x(l_x)$ is excluded from the summation in (2).

Updates in time k (after $\kappa = N$ iterations): Before proceeding from frame k to the next frame $k+1$, the term $\alpha_k(\mathbf{x}_k)$ is obtained after the total number of $\kappa = N$ iterations by the forward recursion [8], [33]

$$\alpha_k(\mathbf{x}_k) = \sum_{\mathbf{x}_{k-1}} \gamma_k(\mathbf{x}_k, \mathbf{x}_{k-1}) \cdot \alpha_{k-1}(\mathbf{x}_{k-1}) \quad (3)$$

with the innovation

$$\gamma_k(\mathbf{x}_k, \mathbf{x}_{k-1}) = P(\mathbf{x}_k | \mathbf{x}_{k-1}) \cdot \exp \sum_{l=1}^w \frac{x_k(l)}{2} \cdot L_{\text{SDSD}}^{[\text{input}],N}(x_k(l)). \quad (4)$$

As initial values serve $\alpha_0(\mathbf{x}_0) = P(\mathbf{x})$ (probability distribution of \mathbf{x}).

After several iterative refinements of $L_{\text{CD}}^{[\text{ext}],\kappa}(x)$ and $L_{\text{SDSD}}^{[\text{ext}],\kappa}(x)$, individual estimates of \hat{v}_k are obtained by MMSE estimation on parameter level [3], [8].

III. EXIT CHART ANALYSIS FOR ISCD

A. EXIT Charts for ISCD

For the analysis and the prediction of the convergence behavior of iterative Turbo processes, the EXIT chart (extrinsic information transfer chart) analysis tool has been proposed in [19]. In what follows, we briefly review the EXIT chart approach. For a thorough description of EXIT charts, we refer the reader to [19].

In an EXIT chart each constituent decoder of the Turbo process is represented by an EXIT characteristic. For this purpose, the mutual information measure $\mathcal{I}(\cdot; \cdot)$ is applied to the input/output relation of each individual decoder. For the constituent decoders of an ISCD scheme we have:

- SISO channel decoding:

$$\mathcal{I}_{\text{CD}}^{[\text{apri}]} = \mathcal{I}(x; L_{\text{SDSD}}^{[\text{ext}]}(x)) \rightarrow \mathcal{I}_{\text{CD}}^{[\text{ext}]} = \mathcal{I}(x; L_{\text{CD}}^{[\text{ext}]}(x))$$

- Soft-decision source decoding:

$$\mathcal{I}_{\text{SDSD}}^{[\text{apri}]} = \mathcal{I}(x; L_{\text{CD}}^{[\text{ext}]}(x)) \rightarrow \mathcal{I}_{\text{SDSD}}^{[\text{ext}]} = \mathcal{I}(x; L_{\text{SDSD}}^{[\text{ext}]}(x)).$$

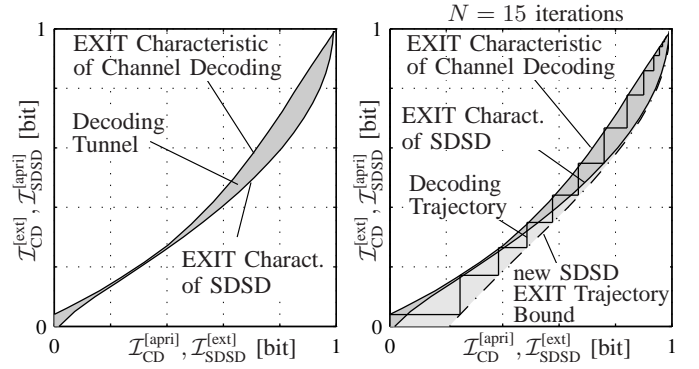


Fig. 2. Exemplary EXIT charts of ISCD at a channel condition of $E_s/N_0 = -4.0$ dB and a temporal parameter correlation of $\rho = 0.9$. Left subplot: EXIT characteristics and decoding tunnel. Right subplot: measured decoding trajectory for $N = 15$ iterations.

Note that in case of channel decoding the mapping from $\mathcal{I}_{\text{CD}}^{[\text{apri}]}$ to $\mathcal{I}_{\text{CD}}^{[\text{ext}]}$ depends on the channel quality E_s/N_0 , because $L(z|y)$ is always implied in the determination of $L_{\text{CD}}^{[\text{ext}]}(x)$ (see Fig. 1). Figure 2 (left subplot) depicts an exemplary EXIT chart for ISCD at a channel condition $E_s/N_0 = -4$ dB for the setup denoted Config. B, to be discussed in detail in Section IV.

The open *decoding tunnel* indicates that the system might converge after a certain number of iterations. The measured *decoding trajectory* is given in the right subplot for Fig. 2. In this example, convergence is achieved after $N = 15$ iterations. The decoding trajectory should reach the upper right corner of the EXIT chart. The decoding trajectory is measured in the actual ISCD system configurations, while the characteristics of the source and channel decoders are measured independently.

From the EXIT chart we can usually determine the necessary number of iterations N for convergence. However, the EXIT characteristic of SDSD does not define a reliable bound for the decoding trajectory, as can be seen in the right subplot of Fig. 2. In this example the decoding trajectory *overshoots* the classic EXIT characteristic of SDSD [24], [25].

B. Overshooting Effect

The overshooting (or undershooting) effect can also result from a too small interleaver size, e.g. [19]. However, we have confirmed by simulation that the interleaver size of 3000 bits, used for the example in Fig. 2, is sufficiently large. In our case, the overshooting mismatch is due to the fact that the SDSD exploits inter-frame parameter correlation, i.e., there exist dependencies between consecutive frames. Similar to serially concatenated channel codes (SCCCs), ISCD operates on a frame-by-frame basis, but in contrast to SCCCs, information from the previous frame $k-1$ is exploited in the SDSD (indicated by the factor $\alpha_{k-1}(\mathbf{x}_{k-1})$ in (1)).

The dependency on the previous frame $k-1$ leads to a mismatch when determining the EXIT characteristic and the decoding trajectory. This is visualized in Fig. 3. The increasing gray scales in Fig. 3-b) illustrate the increasing reliabilities of $\alpha_{k-1}(\mathbf{x}_{k-1})$ for the different iterations κ .

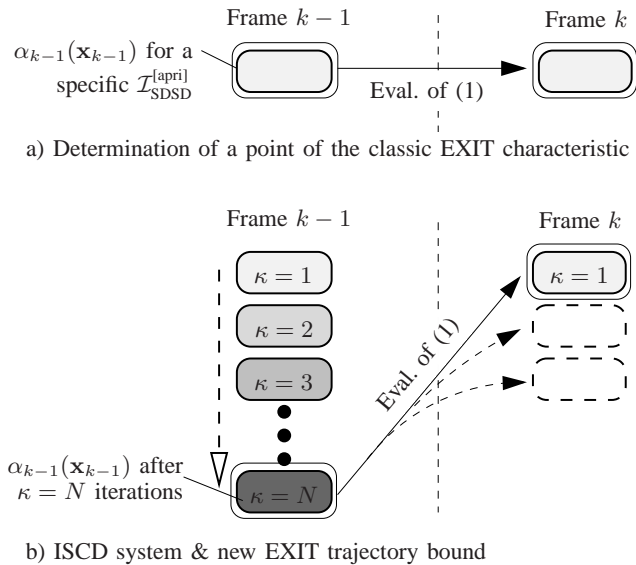


Fig. 3. Illustrations for the determination of the classic EXIT characteristic and the new trajectory bound

The classic EXIT characteristic is *computed* using (1), (4) and (3), with the *same* level of reliability in frame $k-1$ and in frame k (same gray scale in Fig. 3-a).

In contrast, the *measured* ISCD decoding trajectory is based on *different* levels of reliability, as indicated by the different gray scales in Fig. 3-b). The $\alpha_{k-1}(\mathbf{x}_{k-1})$ at frame $k-1$ are more reliable than the $\alpha_k(\mathbf{x}_k)$. The difference becomes smaller with increasing iteration counter κ .

If the ISCD system has fully converged at time instant $k-1$, the input L -values $L_{\text{SDSD}}^{\text{[input],N}}(x)$ at the final iteration ($\kappa = N$) can be considered as perfectly reliable ($\mathcal{I}_{\text{CD}}^{\text{[ext]}} \rightarrow 1$ bit). In this case, the innovation (4) at time $k-1$ becomes perfectly reliable leading to perfectly reliable $\alpha_{k-1}(\mathbf{x}_{k-1})$ (which are evaluated by (3) using $\alpha_{k-2}(\mathbf{x}_{k-2})$). Those highly reliable $\alpha_{k-1}(\mathbf{x}_{k-1})$ are used in the next frame k to determine the extrinsic information using (1).

C. New Trajectory Bound

Hence, for a better prediction of the decoding trajectory of ISCD, we have to extend the classic approach for computing the EXIT characteristic [19], [25]. This extension has to take into account the different levels of reliability.

Initially, we assume that the iterative process has led to $\mathcal{I}_{\text{SDSD,final}}^{\text{[apri]}} \approx 1$ bit, i.e., it has converged. This may be considered as error-free feed-“forward” from preceding frames to the present one.

The first step in the computation of the EXIT trajectory bound is identical to the computation of the classic EXIT characteristic. After executing SDSD for frame k we have to prepare the decoder for the next frame $k+1$: The update of $\alpha_k(\mathbf{x}_k)$ according to (3) has to be executed. In order to take into account the error-free feed-“forward”, we set $\alpha_k(\mathbf{x}_k) = 1$ if \mathbf{x}_k corresponds to the transmitted bit pattern and $\alpha_k(\mathbf{x}_k) = 0$ for all $|\mathcal{V}| - 1$ other potential bit patterns. This emulates the behavior of the converged system. The so-computed novel characteristic can be taken as upper bound for

the decoding trajectory and will be denoted by *EXIT trajectory bound*.

If the SDSD and channel decoder characteristic intersect or if the iterative process does not fully converge, we cannot use the error-free feed-“forward” assumption. In this case, we generate $L_{\text{SDSD}}^{\text{[input],N}}(x)$ following a Gaussian distribution with variance σ_a^2 and mean μ_a which represent the intersection point $\mathcal{I}_{\text{SDSD,inters}}^{\text{[apri]}}$ according to $\sigma_a = J^{-1}(\mathcal{I}_{\text{SDSD,inters}}^{\text{[apri]}})$ and $\mu_a = \sigma_a^2/2$ [19]. These L -values are solely used to update $\alpha_k(\mathbf{x}_k)$ via (3) and (4). An example of this case is given in Config. A in Sec. IV.

The new EXIT trajectory bound is depicted in Fig. 2 for Config. B (see below). It can be seen that the decoding trajectory is delimited by the channel decoder EXIT characteristic and the new SDSD EXIT trajectory bound. Note that the new EXIT trajectory bound does not provide a sufficient condition for convergence. The convergence condition of an open decoding tunnel between the classic EXIT characteristics still has to be fulfilled. The EXIT trajectory bound however indicates that, although only a very narrow decoding tunnel is present, a smaller number iterations as expected is required for convergence in the real ISCD system.

Finally, it should be mentioned that the reason for the overshooting effect lies in the inter-frame parameter correlation. The proposed extension of the EXIT characteristic is only needed if ISCD is configured for exploiting this correlation.

IV. EXIT CHART BASED SYSTEM DESIGN

Most communication systems in service today have been designed for non-iterative receivers. However, in [4]–[6] it has been shown that even in these systems, improved error correcting and parameter reconstructing capabilities can be achieved by using ISCD at the receiver. Larger gains can be realized with especially optimized settings, which require some modifications of the transmitter. The optimization of the index assignment and channel encoding (see Fig. 1) for ISCD has been extensively studied in the literature, e.g., [8], [24], [34]. We choose as a starting point for the EXIT chart based system design the following Config. A which we have proposed in [8].

For all Configs. A-D, we assume that the bit budget on the transmission link is fixed to $(Mw)/r_{\text{CC}}$ (plus some terminating bits). In addition, the index assignment and the channel code shall be designed such that the EXIT characteristics of source and channel decoding provide the utmost open decoding tunnel. In the simulation examples, we assume a correlation of $\rho = 0.9$ or less. Such high correlation values have been observed in typical speech codecs, see, e.g., [3], [35], [36].

A. Reference Design – Config. A

After Lloyd-Max quantization (LMQ) of the source codec parameters to $w = 3$ bits, index assignment and bit mapping are carried out according to the EXIT optimized index assignment² which we have proposed in [8] and which maximizes $\mathcal{I}_{\text{SDSD,max}}^{\text{[ext]}}$ (the anchor point for the EXIT characteristic

²Optimized index assignments show some similarities with optimized constellations in modulation, see e.g., [37]

of SDSD). An S -random bit interleaver Π is applied to a single frame. Finally, the resulting bit patterns are channel encoded by a terminated, rate $1/2$ recursive non-systematic convolutional code with $\mathbf{G} = (\frac{15}{17}, \frac{13}{17})_8$.

B. Redundant Index Assignments and Bit Rate Allocation

The findings in [21], [38], [39] indicate that the inner code of a serially concatenated system should be of rate $r_{CC}^* = 1$ if iterative, Turbo-like decoding is employed. In the context of ISCD, a rate-1 recursive systematic code with partial puncturing of the systematic bits has been introduced in [40], in order to allocate more bits to source coding.

The spare bit budget due to $r_{CC}^* = 1$ can either be utilized for quantization with higher resolution (increased number $|\mathbb{V}^*|$ of quantizer levels) or for a redundant index assignment with regard to higher error robustness (number of data bits $w^* > \log_2 |\mathbb{V}|$), or both ($w^* > \log_2 |\mathbb{V}^*|$). In the present and the succeeding Sections IV-B and IV-C, we focus on the redundant index assignment. In Section IV-D we address the quantization with higher resolution in terms of a multi-mode scheme.

Several powerful redundant index assignments based on block codes of rate $r_{IA} = w/w^*$, with $w^* > w$, have been proposed [17], [26]. Under certain conditions, even a simple single parity check code with $w^* = w + 1$ can be sufficient [17], [22], [23], [26]. The relevant design criterion is a minimum Hamming distance of $d_{\min} \geq 2$ between the index bit patterns \mathbf{x} , such that the EXIT characteristic of SDSD can reach the theoretically maximum value $\mathcal{I}_{\text{SDSD,max}}^{\text{[ext]}} = \mathcal{H}(x)$ [17], [22], [26]. The redundancy introduced by the a block code is exploited in the SDSD.

Figure 4 shows a comparison of this setup (Config. B) with the reference design (Config. A). As performance criterion serves the parameter SNR, i.e., the signal-to-noise ratio between unquantized parameters v and reconstructed parameters \hat{v} . We use a redundant index assignment consisting of $w = 3$ bit natural binary index assignment followed by a systematic $(6, 3)$ block code [26]. Thus, the block coded bit patterns \mathbf{x} are of length $w^* = 2w$. The rate $r_{CC}^* = 1$ convolutional code uses the generator polynomial $\mathbf{G} = (\frac{10}{17})_8$.

The parameter SNR curves of Config. A are reproduced as dashed lines. The solid lines and the upper EXIT chart depict the results for the given setup with the rate $r_{CC}^* = 1$ convolutional code. It can be seen that (at $E_s/N_0 = -4.0$ dB) the ISCD system according to Config. A suffers from an intersection of the EXIT characteristics at $(\mathcal{I}_{\text{SDSD}}^{\text{[ext]}}, \mathcal{I}_{\text{CD}}^{\text{[ext]}}) \approx (0.75, 0.96)$ due to the anchor point of the SDSD characteristic at $\mathcal{I}_{\text{SDSD,max}}^{\text{[ext]}} = 0.79$. In contrast, the system according to Config. B does not suffer from the intersection anymore. In comparison to Config. A, the maximum SNR of 14.6 dB, which is due to the quantization noise $E\{|v - \hat{v}|^2\}$, can be maintained for lower channel SNRs. However, for $E_s/N_0 < -4.2$ dB, Config. A achieves a higher SNR than Config. B.

For both configurations, the new EXIT trajectory bound allows a precise prediction of the number of iterations necessary to reach the upper right corner (or the intersection, respectively) in the EXIT chart (see the sub-plot in the right part of Fig. 4).

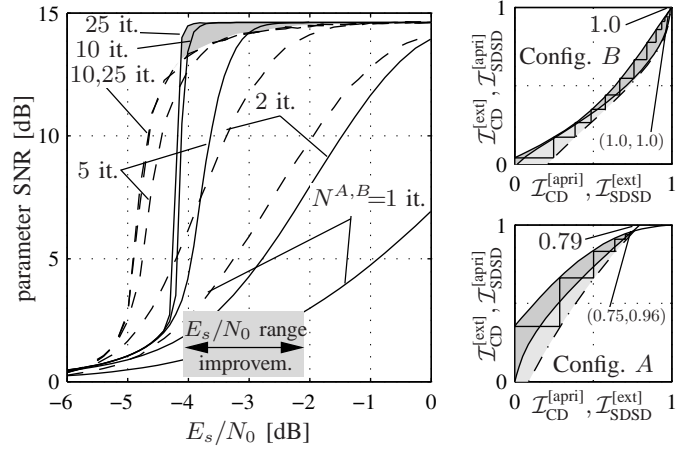


Fig. 4. Simulation results for Configs. A (dashed) and B (solid). Correlation $\rho = 0.9$, $M = 500$ parameters per frame, code book size $|\mathbb{V}| = 8$. Config. A: $r_{CC} = 1/2$ channel code. Config. B: $r_{CC}^* = 1$ channel code.

C. Irregular Index Assignments & Unequal Error Protection

The concept of redundant index assignments can be extended towards so-called irregular index assignments, following the idea of irregular codes [20], [21].

Instead of using the same redundant index assignment $\mathbf{x}_m = \Phi(\bar{v}_m)$ for all $m = 1, \dots, M$ quantized source codec parameters \bar{v}_m a set of different redundant index assignments with different rates $r_{IA,m} = w_m/w_m^*$ is used. However, the total number of bits for a complete bit sequence $\underline{\mathbf{x}}$ remains the same. The primary motivation for irregular index assignments is that an EXIT characteristic for SDSD can be constructed which matches the channel decoder characteristic considerably well. The resulting EXIT characteristic is the weighted sum over all EXIT characteristics of the sub-components. We have applied the concept of irregular codes for the context of ISCD in [27] while a similar principle has been proposed for ISCD with VLCs in [41].

The irregular index assignment is found by solving the following optimization problem [20], [27]:

$$\mathbf{a}_{\text{opt}} = \arg \min_{\mathbf{a}} \|\mathbf{C}\mathbf{a} - \mathbf{d}\|_2 \quad (5)$$

subject to

$$\mathbf{C}\mathbf{a} \succ \mathbf{d} \quad (6)$$

$$\mathbf{r}_{IA}^T \mathbf{a} = r_{IA,\text{target}} \quad (7)$$

$$\sum_{j=1}^F a_j = 1 \quad \text{and} \quad 0 \leq a_j \leq 1. \quad (8)$$

The matrix \mathbf{C} (with $\dim \mathbf{C} = S \times F$) contains S sample points of each of the F distinct SDSD EXIT characteristics of the different index assignments. The vector \mathbf{d} contains S sample points of the inverse channel decoder EXIT characteristic and $\mathbf{r}_{IA} = (r_{IA,1}, \dots, r_{IA,F})^T$ is a column vector containing the rates of the different utilized index assignments. The symbol “ \succ ” in (6) requires that all elements of the left-hand side vector are greater than the corresponding element of the vector on the right-hand side.

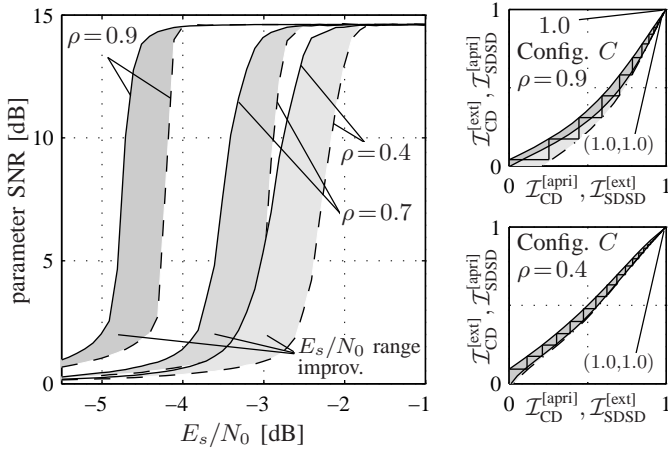


Fig. 5. Simulation results for Configs. *B* (dashed) and *C* (solid). Correlation $\rho \in \{0.9; 0.7; 0.4\}$, $M = 500$ parameters per frame, code book size $|\mathbb{V}| = 8$. Config. *B*: regular index assignment. Config *C*: irregular index assignment, $N^B = N^C = 25$ iterations

The outcome of the optimization are weights \mathbf{a}_{opt} which denote the fraction of bits (after index assignment) to be encoded with each distinct assignment. Constraint (6) ensures that an open EXIT decoding tunnel is present while constraint (7) guarantees that the resulting rate of the index assignment is as desired [20]. The problem (5)-(8) can be solved numerically [20], [21]. Using \mathbf{a} , the number of parameters $M_{w_j^*}$ to be encoded by the index assignment of rate $r_{\text{IA},j} = \frac{w}{w_j^*}$ is given by [27]

$$M_{w_j^*} = \text{rnd} \left[\frac{r_{\text{IA},j}}{r_{\text{IA},\text{target}}} \right] = \text{rnd} \left[\frac{a_j w M}{w_j^* \cdot r_{\text{IA},\text{target}}} \right], \quad (9)$$

with rnd denoting rounding to ensure $\sum_j M_{w_j^*} = M$.

A simulation example is shown in Fig. 5 with Config. *B* (dashed curves) as reference. Instead of the block coded index assignment an irregular index assignment consisting of three constituent index assignments of length $w^* \in \{4, 5, 12\}$ bit, has been used. Each of these constituent index assignments is applied to a certain number of parameters, $M_{w^*} \in \{193, 208, 99\}$; the index assignment with $w^* = 4$ is used $M_{w^*} = 193$ times and so on. The overall number of bits x in the bit sequence $\underline{\mathbf{x}}$ remains to be $\frac{wM}{r_{\text{IA},\text{target}}} = \sum w_j^* M_{w_j^*} = 3000$. Even though the irregular index assignment has once been optimized for $\rho = 0.9$, it yields gains ranging between 0.5 and 1 dB in terms of channel quality for different values of ρ .

In the right part of Fig. 5, EXIT charts of the ISCD system with irregular index assignments are given for $\rho = 0.9$ ($E_s/N_0 = -4$ dB) and $\rho = 0.4$ ($E_s/N_0 = -2.5$ dB). The EXIT trajectory bound (dash-dotted lines) of the irregular index assignment is obtained by a weighted superposition of the different constituent trajectory bounds. For $\rho = 0.4$, the overshooting effect is less pronounced due to the lower inter-frame correlation and the classic EXIT characteristic already presents a proper limit for the decoding trajectory.

Besides finding the optimal EXIT characteristic of SSDS, irregular index assignments also lead to inherent *unequal error protection* (UEP). Those parameters that are encoded using a

high-rate index assignment are more prone to decoding errors than the ones encoded using lower-rate index assignments. This effect can be explicitly taken into account in the design of an ISCD scheme by adding an additional constraint to (5). Let us assume that at least $M_{\text{high}} < M$ parameters are of high importance and shall be encoded using low-rate assignments, the constraint

$$\sum_{j=1}^{j_{\text{lim}}} M_{w_j^*} \approx \sum_{j=1}^{j_{\text{lim}}} a_j \frac{wM}{w_j^* \cdot r_{\text{IA},\text{target}}} \geq M_{\text{high}} \quad (10)$$

can be added to the optimization problem (5)-(8), with j_{lim} defined such that $r_{\text{IA},j} = \frac{w}{w_j^*} \leq r_{\text{IA},\text{target}}, \forall j \in \{1, \dots, j_{\text{lim}}\}$. This scheme presents an alternative to the UEP scheme based on ISCD as proposed in [42].

D. Multi-Mode Scheme

In Sections IV-B and IV-C, the rate $r_{\text{CC}} = 1$ channel code leaves a spare bit budget which has been utilized for the redundant index assignment. As an alternative, (parts of) the spare bit budget can be exploited to lower the quantization noise. Any number $|\mathbb{V}^*|$ of quantizer reproduction levels \bar{v} is possible as long as $|\mathbb{V}^*| \leq 2^{w^*}$ [26], leading to a trade-off between quantization with higher resolution and redundant index assignment with regard to higher error robustness (see Sec. IV-B). Different realizations of this trade-off can be used to construct a multi-mode system with dynamically splitting the available bit rate between quantization and error protection according to the instantaneous quality of the radio channel. With this channel quality dependent adaption of the source and channel coding budgets, we have an iterative pendant to the findings in [43] for the non-iterative case.

Figure 6 shows the simulation results for such a multi-mode system (Config. *D*). The bold curve depicts the parameter SNR envelope for several values of $|\mathbb{V}^*|$ between 2 and 32 with $N = 25$ iterations each. In contrast to [26], each curve is obtained using specifically optimized irregular index assignments according to Sec. IV-C. Values of $|\mathbb{V}^*| > 32$

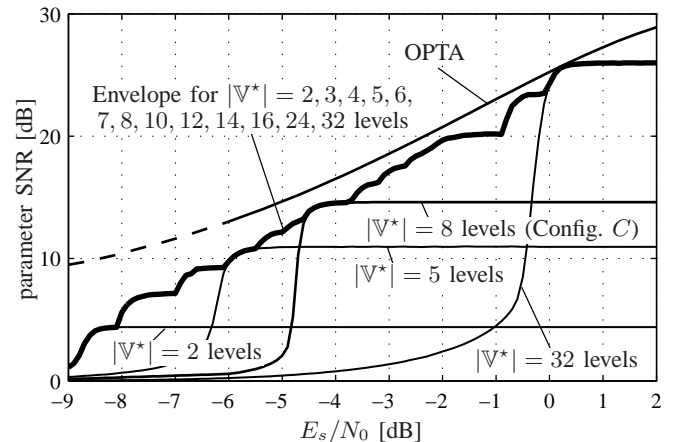


Fig. 6. Simulation results for Config. *D* with $N^D = 25$ iterations as well as the performance bound OPTA. Correlation $\rho = 0.9$, $M = 500$ parameters per frame, code book size $|\mathbb{V}| = 8$.

cannot be used, as for $w^* = 6$ bit, there exists at least one pair of bit patterns with a Hamming distance of $d_{\min} = 1$.

The bold curve represents the parameter SNR of a multi-mode system with perfect adaptation to the instantaneous channel quality. This means that always the specific mode (i.e., the combination of code book \mathbb{V}^* and redundant index assignment $\Phi^*(\cdot)$) will be selected which offers the highest parameter SNR.

In addition, as a reference the *optimum performance theoretically attainable* (OPTA) as defined in [44], [45] is depicted for a scalar Lloyd-Max quantizer (LMQ) and auto-correlated samples ($\rho = 0.9$). It can be seen that the adaptive multi-mode system offers a performance that is very close to the optimum in moderate and good channel conditions. The depicted OPTA limit has been approximated using the low-distortion assumption and is only tight for a parameter SNR > 12.8 dB [44] (the high-distortion regime is indicated by the dashed line in Fig. 6).

In contrast to prior adaptive multi-mode joint source-channel coding systems like the GSM-AMR (adaptive multi-rate) [46], [47], the (inner) channel coding component does not need to be adapted. The number of data bits x provided to the channel encoder is the same for all combinations.

V. CONCLUSIONS

In this article we discussed EXIT chart based system design for ISCD with FLCs. First, we analyzed the overshooting effect of the decoding trajectory which is mainly due to inter-frame parameter correlation. This had not been taken into account in classic EXIT charts so far. We proposed a novel extension to the EXIT chart technique, yielding an EXIT trajectory bound which provides a significantly better limit for the ISCD decoding trajectory. In the second part of the paper, the EXIT chart technique and its new trajectory bound extension have been applied for the design and the analysis of several advanced ISCD system configurations. This includes regular and irregular redundant index assignments, which yield significant performance improvements in terms of parameter SNR. We have shown how unequal error protection capabilities can be incorporated into the system design. Finally, a multi-mode ISCD system which operates close to the theoretical OPTA limit has been presented.

ACKNOWLEDGMENT

The authors would like to thank the anonymous reviewers for many inspiring and fruitful comments, which helped improving the quality of the manuscript.

REFERENCES

- [1] K. Sayood and J. C. Borkenhagen, "Use of Residual Redundancy in the Design of Joint Source/Channel Coders," *IEEE Trans. Commun.*, vol. 39, no. 6, pp. 838–846, Jun. 1991.
- [2] J. Hagenauer, "Source-Controlled Channel Decoding," *IEEE Trans. Commun.*, vol. 43, no. 9, pp. 2449–2457, Sep. 1995.
- [3] T. Fingscheidt and P. Vary, "Softbit Speech Decoding: A New Approach to Error Concealment," *IEEE Trans. Speech Audio Process.*, vol. 9, no. 3, pp. 240–251, Mar. 2001.
- [4] N. Görtz, "Iterative Source-Channel Decoding using Soft-In/Soft-Out Decoders," in *IEEE ISIT*, Sorrento, Italy, Jun. 2000, p. 173.
- [5] T. Hindelang, T. Fingscheidt, R. V. Cox, and N. Seshadri, "Combined Source/Channel (De-)Coding: Can A Priori Information Be Used Twice?" in *IEEE ISIT*, Sorrento, Italy, Jun. 2000, p. 266.
- [6] M. Adrat, P. Vary, and J. Spittka, "Iterative Source-Channel Decoder Using Extrinsic Information from Softbit-Source Decoding," in *IEEE ICASSP*, vol. IV, Salt Lake City, Utah, USA, May 2001, pp. 2653–2656.
- [7] N. Görtz, "On the Iterative Approximation of Optimal Joint Source-Channel Decoding," *IEEE J. Sel. Areas Commun.*, vol. 19, no. 9, pp. 1662–1670, Sep. 2001.
- [8] M. Adrat and P. Vary, "Iterative Source-Channel Decoding: Improved System Design Using EXIT Charts," *EURASIP J. Appl. Signal Process.; Special Issue Turbo Process.*, vol. 2005, no. 6, pp. 928–941, May 2005.
- [9] T. Hindelang, "Source-Controlled Channel Encoding and Decoding for Mobile Communications," Ph.D. dissertation, Institute of Comm. Engineering, Munich University of Technology, ISBN 3-18-369510-3, 2001.
- [10] J. Hagenauer, E. Offer, and L. Papke, "Iterative Decoding of Binary Block and Convolutional Codes," *IEEE Trans. Inf. Theory*, vol. 42, no. 2, pp. 429–445, Mar. 1996.
- [11] J. Kliewer and R. Thobaben, "Iterative Joint Source-Channel Decoding of Variable-Length Codes Using Residual Source Redundancy," *IEEE Trans. Wireless Commun.*, vol. 4, no. 3, pp. 919–929, May 2005.
- [12] R. Thobaben, "Iterative Quellen- und Kanaldecodierung für Codes variabler Länge," Ph.D. dissertation, Institute for Circuit and System Theory, University of Kiel, ISBN 978-3-8322-6351-5, 2007, (in German).
- [13] C. Guillemot and P. Siohan, "Joint Source-Channel Decoding of Variable-Length Codes with Soft Information: A Survey," *EURASIP J. Appl. Signal Process.; Special Issue Turbo Process.*, pp. 906–927, May 2005.
- [14] R. Perkert, M. Kaindl, and T. Hindelang, "Iterative Source and Channel Decoding for GSM," in *IEEE ICASSP*, vol. 4, Salt Lake City, Utah, USA, May 2001, pp. 2649–2652.
- [15] N. S. Othman, M. El-Hajjar, O. Alamri, and L. Hanzo, "Soft-Bit Assisted Iterative AMR-WB Source-Decoding and Turbo-Detection of Channel-Coded Differential Space-Time Spreading Using Sphere Packing Modulation," in *IEEE VTC-Spring*, Dublin, Ireland, Apr. 2007.
- [16] J. Kliewer and N. Görtz, "Iterative Source-Channel Decoding for Robust Image Transmission," in *IEEE ICASSP*, vol. 3, Orlando, Florida, USA, May 2002, pp. 2173–2176.
- [17] J. Kliewer, N. Görtz, and A. Mertins, "Iterative Source-Channel Decoding with Markov Random Field Source Models," *IEEE Trans. Signal Process.*, vol. 54, no. 10, pp. 3688–3701, Oct. 2006.
- [18] Nasruminallah, M. El-Hajjar, N. S. Othman, A. P. Quang, and L. Hanzo, "Over-Complete Mapping Aided, Soft-Bit Assisted Iterative Unequal Error Protection H.264 Joint Source and Channel Decoding," in *IEEE VTC-Fall*, Calgary, Canada, Sep. 2008.
- [19] S. ten Brink, "Convergence Behavior of Iteratively Decoded Parallel Concatenated Codes," *IEEE Trans. Commun.*, vol. 49, no. 10, pp. 1727–1737, Oct. 2001.
- [20] M. Tüchler and J. Hagenauer, "EXIT Charts of Irregular Codes," in *Proceedings of Conference on Information Sciences and Systems (CISS)*, Princeton, NJ, USA, Mar. 2002.
- [21] M. Tüchler, "Design of Serially Concatenated Systems Depending on the Block Length," *IEEE Trans. Commun.*, vol. 52, no. 2, pp. 209–218, Feb. 2004.
- [22] A. Q. Pham, L. L. Yang, and L. Hanzo, "Iterative Source and Channel Decoding Using Over-Complete Source Mapping," in *IEEE VTC-Fall*, Baltimore, MD, USA, Sep. 2007, pp. 1072–1076.
- [23] R. Thobaben, "A New Transmitter Concept for Iteratively-Decoded Source-Channel Coding Schemes," in *IEEE Workshop on Signal Processing Advances in Wireless Communications (SPAWC)*, Helsinki, Finland, Jun. 2007.
- [24] T. Clevorn, P. Vary, and M. Adrat, "Parameter SNR Optimized Index Assignments and Quantizers Based on First Order A Priori Knowledge for Iterative Source Channel Decoding," in *Conf. Inform. Sciences and Systems (CISS)*, Princeton, NJ, USA, Mar. 2006.
- [25] M. Adrat, M. Antweiler, L. Schmalen, P. Vary, and T. Clevorn, "On the Overshooting Effect in EXIT Charts of Iterative Source-Channel Decoding," in *IEEE ICC*, Cape Town, South Africa, May 2010.
- [26] T. Clevorn, P. Vary, and M. Adrat, "Iterative Source-Channel Decoding using Short Block Codes," in *IEEE ICASSP*, Toulouse, France, May 2006.
- [27] L. Schmalen, P. Vary, T. Clevorn, and B. Schotsch, "Efficient Iterative Source-Channel Decoding Using Irregular Index Assignments," in *Proceedings of International ITG Conference on Source and Channel Coding (SCC)*, Ulm, Germany, Jan. 2008.

- [28] C. Poulliat, D. Declercq, C. Lamy-Bergot, and I. Fijalkow, "Analysis and Optimization of Irregular LDPC Codes for Joint Source-Channel Decoding," *IEEE Commun. Lett.*, vol. 9, no. 12, pp. 1064–1066, Dec. 2005.
- [29] K. Lakovic, T. Tian, and J. Villasenor, "Iterative Decoder Design for Joint Source-Channel LDPC Coding," in *EUROCON*, Belgrade, Serbia and Montenegro, Nov. 2005.
- [30] X. Jaspas and L. Vandendorpe, "Joint Source-Channel Codes Based on Irregular Turbo Codes and Variable Length Codes," *IEEE Trans. Commun.*, vol. 56, no. 11, pp. 1824–1835, Nov. 2008.
- [31] K. Lakovic and J. Villasenor, "Combining Variable Length Codes and Turbo Codes," in *IEEE VTC-Spring*, Birmingham, AL, USA, May 2002.
- [32] J. Kliewer, A. Huebner, and D. J. Costello, "On the Achievable Extrinsic Information of Inner Decoders in Serial Concatenation," in *IEEE ISIT*, Jul. 2006, pp. 2680–2684.
- [33] L. R. Bahl, J. Cocke, F. Jelinek, and J. Raviv, "Optimal Decoding of Linear Codes for Minimizing Symbol Error Rate," *IEEE Trans. Inf. Theory*, vol. 10, pp. 284–287, Mar. 1974.
- [34] N. Görtz, "Optimization of Bit Mappings for Iterative Source-Channel Decoding," in *Int. Symp. on Turbo Codes & Related Topics*, Brest, France, Sep. 2003, pp. 255–258.
- [35] F. Alajaji, N. Phamdo, and T. Fuja, "Channel Codes That Exploit the Residual Redundancy in CELP-Encoded Speech," *IEEE Trans. Speech Audio Process.*, vol. 4, no. 5, pp. 325–336, Sep. 1996.
- [36] T. Fazel and T. Fuja, "Robust Transmission of MELP-Compressed Speech: An Illustrative Example of Joint Source-Channel Decoding," *IEEE Trans. Commun.*, vol. 51, no. 6, pp. 973–982, Jun. 2003.
- [37] P. Robertson and T. Wörz, "Bandwidth-efficient Turbo Trellis-coded Modulation using Punctured Component Codes," *IEEE J. Sel. Areas Commun.*, vol. 16, no. 2, pp. 206–218, Feb. 1998.
- [38] S. Benedetto, D. Divsalar, G. Montorsi, and F. Pollara, "Serial Concatenation of Interleaved Codes: Performance Analysis, Design, and Iterative Decoding," *IEEE Trans. Inf. Theory*, vol. 44, no. 3, pp. 909–926, May 1998.
- [39] A. Ashikhmin, G. Kramer, and S. ten Brink, "Extrinsic Information Transfer Functions: Model and Erasure Channel Properties," *IEEE Trans. Inf. Theory*, vol. 50, no. 11, pp. 2657–2673, Nov. 2004.
- [40] J. Kliewer and R. Thobaben, "On Iterative Source-Channel Decoding for Variable-Length Encoded Markov Sources Using a Bit-level Trellis," in *IEEE Workshop on Signal Processing Advances in Wireless Communications (SPAWC)*, Rome, Italy, Jun. 2003.
- [41] R. G. Maunder, J. Wang, S. X. Ng, L.-L. Yang, and L. Hanzo, "On the Performance and Complexity of Irregular Variable Length Codes for Near-Capacity Joint Source and Channel Coding," *IEEE Trans. Wireless Commun.*, vol. 7, no. 4, pp. 1338–1347, Apr. 2008.
- [42] A. Q. Pham, L. L. Yang, and L. Hanzo, "Unequal Error Protection Irregular Over-Complete Mapping for Wavelet Coded Wireless Video Telephony Using Iterative Source and Channel Decoding," in *IEEE Wireless Communications & Networking Conference (WCNC)*, Las Vegas, NV, USA, Mar. 2008.
- [43] B. Hochwald and K. Zeger, "Tradeoff Between Source and Channel Coding," *IEEE Trans. Inf. Theory*, vol. 43, no. 5, pp. 1412–1424, Sep. 1997.
- [44] T. Clevorn, L. Schmalen, P. Vary, and M. Adrat, "On the Optimum Performance Theoretically Attainable for Scalarly Quantized Correlated Sources," in *Intern. Symp. Inf. Theory and its Applications (ISITA)*, Seoul, Korea, Oct. 2006.
- [45] N. Görtz, *Joint Source-Channel Coding of Discrete-Time Signals with Continuous Amplitudes*. Imperial College Press, Sep. 2007, ISBN 1-86094-845-6.
- [46] ETSI, "Adaptive Multi-Rate AMR Speech Transcoding," ETSI, Tech. Rep. GSM 06.90, 1998.
- [47] —, "Digital cellular telecommunications system (Phase 2+); Channel coding," ETSI, Tech. Rep. GSM 05.03, 1999.